ISBN: 978-3-95450-233-2 ISSN: 2673-5504 doi:10.18429/JACoW-SRF2021-TUPTEV001

RF EXPERIENCE FROM 6 YEARS OF ELBE SRF-GUN II OPERATION

A. Arnold†, P. Lu, S. Ma, P. Murcek, A. Ryzhov, J. Schaber, J. Teichert, R. Xiang
HZDR, Dresden, Germany
G. Ciovati, P. Kneisel, H. Vennekate, JLab, Newport News, VA, USA

Abstract

At the electron accelerator for beams with high brilliance and low emittance (ELBE), the second version of a superconducting radio-frequency (SRF) photoinjector was brought into operation in 2014. After a period of commissioning, a gradual transfer to routine operation took place in 2017 and 2018, so that now more than 3400h of user beam have already been generated since 2019. During this time, a total of 20 cathodes (2 Cu, 12 Mg, 6 Cs2Te) were used, but no serious cavity degradation was observed. In this paper, we summarize the operational experience of the last 6 years of SRF gun operation, with special emphasis on main RF properties of the gun cavity.

INTRODUCTION

At the superconducting (SC) electron linear accelerator of the ELBE radiation facility [1] a new superconducting electron photo injector has been installed in May 2014. This SRF gun II is replacing the previous one which had been in successful test operation from 2007 until April 2014. Although SRF gun I could not reach the design specifications, it was successfully operated for R&D purposes and also some dedicated user experiments at the ELBE accelerator had been done [2].

For SRF gun II a new niobium cavity has been built, treated and tested at JLab [3]. At the same time a new cryomodule has been designed and built at HZDR. In November 2013, the cavity was shipped to HZDR and assembled into the cryomodule. About half a year later, the gun was installed into the ELBE accelerator hall and transferred into routine operation. The main task of SRF gun II is to demostrate an average current up to 1 mA as well as to serve as an electron source for user operation (e.g. THz generation with 200 pC and some 100 kHz of rep. rate).

CRYOMODULE DESIGN

The design of the SRF gun II cryomodule is shown in Fig. 1. Most of the components are similar or even identical to the previous gun [4].

The cryomodule is designed for CW operation of a superconducting Nb cavity cooled down to 2K. For this purpose, the helium vessel is equipped with a 2-phase helium pipe that can handle a heat load of 40 W (or 2g/s). This value is composed by 7 W static loss and up to 33 W dynamic loss. Since the latter is determined by the electrical field inside the cavity in addition an electric heater is used to operate the cryomodule always at the same helium load (or mass flow) regardless of the cavity gradient. This has been proven to be advantageous to achieve a pressure stability of down to 0.1 mbar rms in the whole helium system.

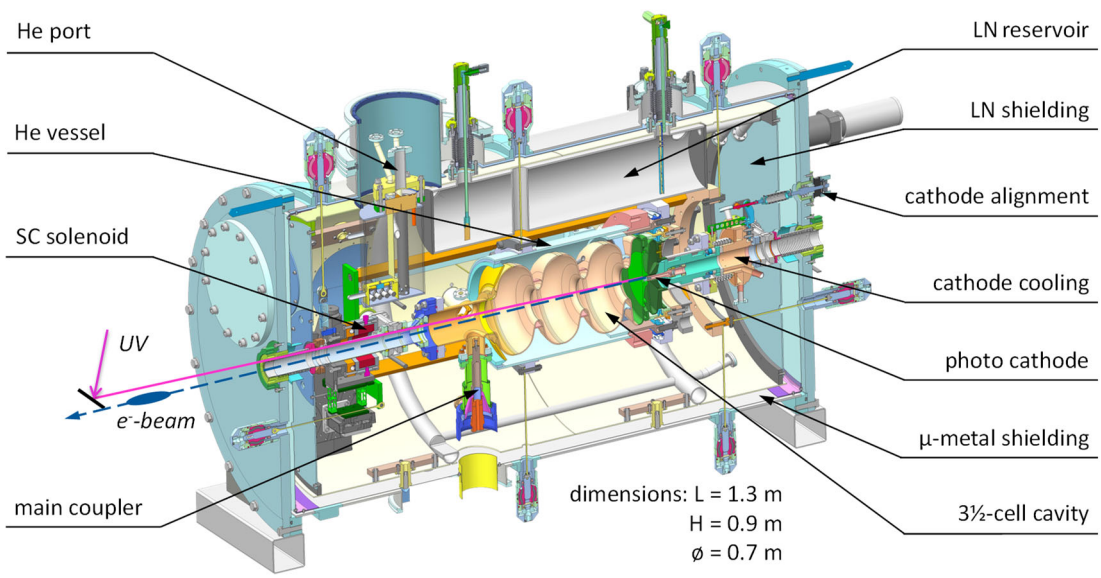

Figure 1: Cross section of the ELBE SRF gun II cryomodule, holding a 3.5 cell gun cavity and a superconducting solenoid at about 70 cm in front of the cathode.

†a.arnold@hzdr.de

ISBN: 978-3-95450-233-2 ISSN: 2673-5504 doi:10.18429/JACoW-SRF2021-TUPTEV001

A liquid nitrogen cooled thermal shield reduces thermal radiation into the helium system. Further insulation is achieved by 20 layers of superinsulation foil surrounding everything at 2K. Thin titanium tension rods hold the complete cold mass in the center of the cryomodule and allow its precise alignment from outside. In order to shield external magnetic fields a warm magnetic shield made from MUMETALL® follows next to the inner wall of the vacuum vessel. Accompanied by consequent avoidance of ferromagnetic materials e.g. by the use of solid copper cables as well as by demagnetization of all components inside the magnetic shield, the achieved magnetic flux in the module is 1-2 µT, and thus makes a second cold shield, enclosing the cavity itself, not necessary. More details can be found elsewhere [5].

The cryomodule itself has a cylindrical shape with 0.7 m diameter and 1.3 m length. Both the liquid helium (LHe) and the liquid nitrogen (LN) port are placed on top of the vessel and provide an isolated feedthrough of the cooling media into the inner of the module. In addition to the helium pot, a second internal reservoir is regularly filled with nitrogen and used to cool the thermal shield, the photocathode cooler and the main power coupler at the same time. The overall static LN load is about 45 W and another 10 W (2 W from cathode and 8 W from RF coupler) result from dynamic losses during CW operation at a gradient of 8 MV/m.

A compact superconducting solenoid is mounted directly in front of the cavity at about 0.7 m from the cathode. A passive magnetic shield out of CRYOPERM® is installed around the solenoid's yoke. As the solenoid is mounted on an x-y-stage it is possible to compensate for misalignment of the geometrical and magnetic axes (see Fig. 2). The steppers of this platform, containing permanent magnets, have also been shielded in order to keep the residual magnetic field at the cavity on a 1 µT level. More details of the SC solenoid design and testing are published elsewhere [6].

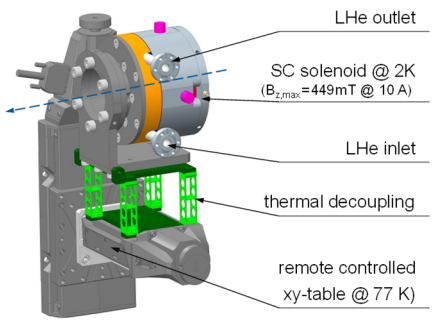

Figure 2: Superconducting solenoid with support frame for thermal decoupling and xy-table for remote positioning.

The photocathode is thermally and electrically isolated from the cavity by a vacuum gap and cooled down with liquid nitrogen. Both allow the use of a normal conducting (NC) photocathodes with high quantum efficiency (QE) such as Cs_2Te but also metal cathodes e.g. Mg in the superconducting environment of the gun. The cathode cooling and support unit was designed for an easy exchange of the cathodes into the cold gun as well as for precise positioning afterwards. Therefore, three rotary feedthroughs at the backside of the module allow for axial cathode movement (±0.6 mm) with respect to the cavity. This allows optimization for best RF focusing but also for radial adjustment of the cathode in the half cell. Additionally, a DC bias up to 7 kV can be applied to the cathode in order to suppress multipacting (MP) that may occur in the gap between cathode and cavity (see Fig. 3).

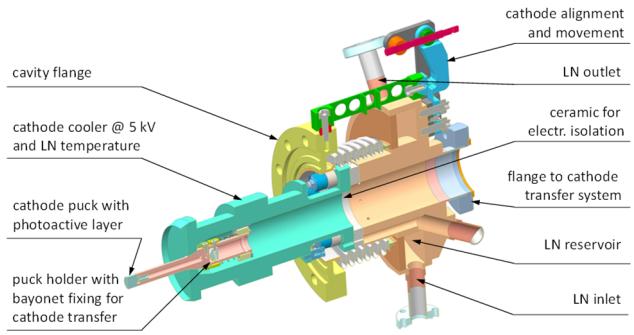

Figure 3: Cathode cooling (LN2) and support unit.

Beside the cavity itself the design is completed by a coaxial fundamental mode power coupler (FPC) and two TESLA type higher order mode (HOM) dampers, all attached to beam pipe at the gun exit. The FPC was developed at HZDR and can handle at least 20kW of CW RF power. The coupling factor (or external Q) is fixed and has to be adjusted before the final assembly by choosing a dedicated length of the tip. Typical values are $6E6<Q_{ext}<3E7$. The cold part of the coupler is composed by a coaxial waveguide those inner and outer conductors are connected to a conical ceramic - the cold window. The cold window separates the beamline vacuum from the coupler vacuum and is cooled with liquid nitrogen.

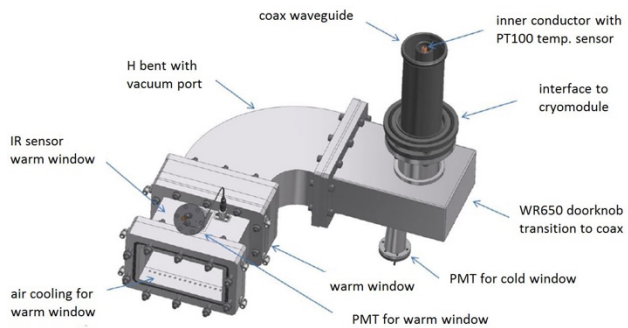

Figure 4: Warm part of the FPC with interlock diagnostic and doorknob waveguide transition.

The warm parts of the coupler and here mainly the so-called Doorknobs realizes the transition between the coaxial and the rectangular waveguide (WR650) used for low loss RF transport. A second warm window made of quartz glass is located in the waveguide and acts as vacuum barrier between coupler vacuum and atmosphere (Fig. 4). To avoid glow discharges a pressure of 1E-7 mbar is realized by a separate turbo molecular pump. In order to protect cold and warm coupler parts in case of unexpected events several measures are realized. Photomultiplier tubes (PMT

ISBN: 978-3-95450-233-2 ISSN: 2673-5504 doi:10.18429/JACoW-SRF2021-TUPTEV001

H5783 or H11901 from Hamamatsu), one for the cold window and one for the warm window are used to detect light discharge. Additionally, the vacuum and the temperature of the inner conductor as well as of the warm window is constantly monitored. Whenever a certain threshold of at least one sensor is exceeded the RF is switched off immediately. A typical shutdown time of <1 ms is realized by the PMTs.

GUN CAVITY

For SRF gun II a new 1.3 GHz niobium cavity was built, treated and tested at JLab. The 1.3 GHz Nb cavity is made of three TESLA like cells and one beta optimized half-cell. A fifth superconducting cell, called choke filter, is surrounding the cathode and prevents RF leakage into the cathode support system. Compared to former version the half-cell was improved by a stiffening structure to reduce Lorentz force detuning and it was tuned to a slightly higher on-axis electric field (80% compared to the three TESLA like cells) to improve beam dynamics [7]. The corresponding electric and magnetic surface fields as well as the on-axis accelerating field of this 3.5 cell cavity are given in Fig. 5.

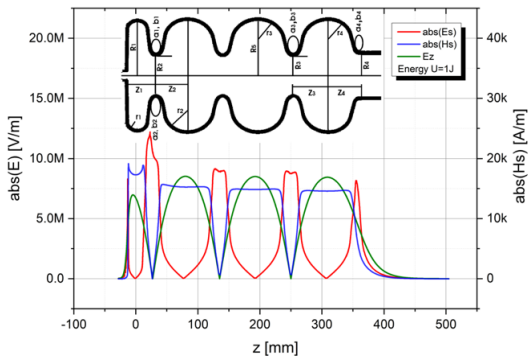

Figure 5: 3.5 cell cavity design and its corresponding electric and magnetic fields for a stored energy of 1 Joule.

In order to evaluate the performance of the cavity it is most common to measure the intrinsic quality (Q_0) as a function of the accelerating gradient (E_{acc}). The cavity had been vertically measured after the treatment in Jefferson Lab in 2013, and then horizontally using a copper cathode during the commission process in 2014. Since then the performance of cavity has been monitored regularly every time after new cathodes (Mg and Cs_2Te) were introduced into the gun. Some selected results are shown in Fig. 6. Compared to the last vertical test at Jefferson Lab the cavity lost about 30% of its performance because of field emission and got even worse after the first introduction of a Cs_2Te cathode. Detailed information about the origin of the limiting field emitter are published elsewhere [8]. Although, the remaining gradient is still higher than that of SRF gun I, this demonstrates the high risk of particle contamination by using NC cathodes in SC cavities. Fortunately, the cavity performance settles at this level and remains constant over the last 6 years of operation despite 20 different Cs_2Te and Mg cathodes introduced into the gun. The main RF parameters are summarized and compared with the design values in Table 1.

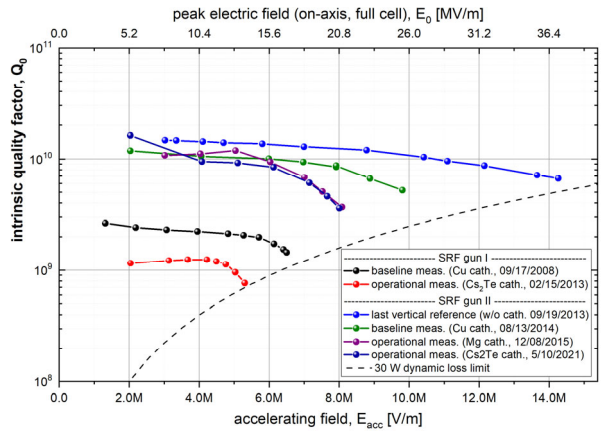

Figure 6: Comparison of Q_0 as a function of E_{acc}. The diagram shows a significant improvement compared to SRF gun I and stable performance over the last 6 years.

Table 1: Comparison between RF Design Parameters and Parameters Achieved during Routine Operation

	Design	Operation
V_{acc}	7.8 MV	4 MV
E_{acc}	15.6 MV/m	8 MV/m
E_{cath}	~0.6xE0=24 MV/m	12-14 M/m [3]
E_0	40 M/m	20.5 M/m
E_{pk}	57 M/m	29 MV/m [1]
H_{pk} (B_{pk})	90000 A/m (110 mT)	46000 A/m (58 mT) [2]
P_{diss}	18 W, (Q0=1e10)	10 W, (Q0=5e9)
L	0.5 m	0.5 m
R/Q	168.1 Ohm	167.9 Ohm
G	224 Ohm	224 Ohm
φ_{launch}	82°	55°
U	22 J	6 J

[1] iris between. half- and TESLA cell
[2] half-cell
[3] depending on cathode length and position

A phenomenon that is closely connected to the cavity performance is the dark current. Here field emitters produce electrons that are able to escape the gun. A part of this electrons pass through the beam line and gain energy in the accelerator. As this increase measurement background of user experiments as well as the radiation level in the bunker, it is worth to analysis the properties of the current and to reduce it as much as possible. However, since this is not the subject of this paper, just a reference to another paper is given [9]. Here we just want to mention that the dark current for a typical cavity gradient of E_{acc} = 8 MV/m is 40-60 nA (depending from cathode).

Another issue is multipacting near the cathode. Free cesium atoms on the shell surface of cathode plug are increasing the secondary electron yield and thus favour electron multiplication in the gap between cathode and cavity. Studies in cooperation with Universities in Rostock and Siegen came to the result that beside several measures the most effective one is to limited the Ø4 mm Cs_2Te layer in the centre of the Ø10mm plug. In combination with a DC bias serious MP could not be observed in the experiments anymore.

ISBN: 978-3-95450-233-2 ISSN: 2673-5504 doi:10.18429/JACoW-SRF2021-TUPTEV001

MECHANICAL PROPERTIES

The cavity is equipped with a double tuning system which means the half-cell can be tuned separately from the rest of the cavity. This is necessary because of the different mechanical stiffness of both parts, but also allows a field flatness adjustment even after the helium vessel welding. A schematic drawing of the tuning concept is shown in Fig. 7.

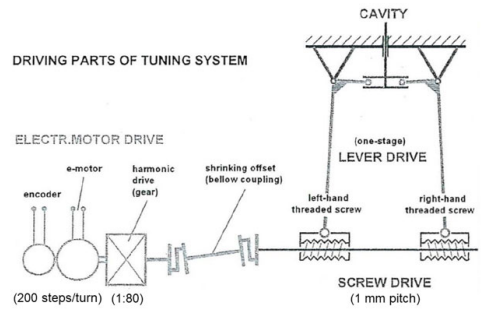

Figure 7: Schematic drawing of the tuning concept.

The tuner consists of a lever gear pair, which is made of titanium (Ti2) and CuNiSi alloy. This guarantees identical thermal expansion properties for tuner, cavity and helium vessel which minimizes frequency detuning due to cooldown. The tuning is realized by both lever arms that are moved against each other on a dry lubricated spindle drive. This cause a length change to the cavity and thus a change in frequency. The spindle drive is coupled via stainless steel bellows and vibration damped rotary vacuum feedthrough almost free from backlash with the drive unit located outside the cryostat. The bellows compensates for axial misalignment and reduces heat transfer to the cavity. The drive unit is mounted outside of the cryostat and consists of a backlash-free Harmonic Drive gear box with a ratio of 1/80 and a stepper motor with 200 steps/turn. Both tuners show an excellent frequency resolution of 0.3 Hz/step (half-cell) as well as 0.8 Hz/step (TESLA cells) and a negligible hysteresis. At the same time the system provides a wide tuning range of almost ±300kHz to compensate for various mechanical tolerances. More details are published here [10].

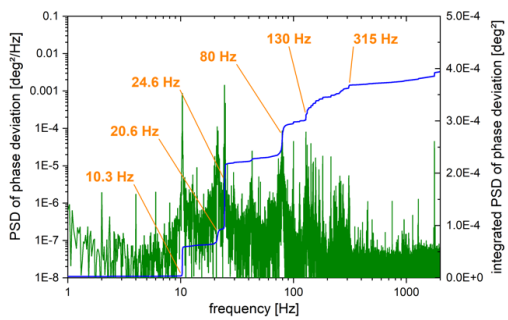

Figure 8: Power spectral density (PSD) of the in loop phase noise of the analog LLRF controller at E_{acc}=9 MV/m.

Further properties that are mainly determined by the design and stiffness of the cavity are microphonics, Lorentz Force (LF) detuning and helium pressure sensitivity. The first is understood as a continuous perturbation of the resonant frequency by external vibrations. This leads to a modulation of amplitude and phase and has to be minimized in a first step by suitable design measures. However, as superconducting cavities prove to be particularly demanding and also sources of vibrations cannot be eliminated or efficiently attenuated along its transport medium, additional compensation by adjusting amplitude and phase using a so-called low-level RF controller is realized (see next section). Signals out of such a feedback loop were used to determine the remaining phase noise and its frequency spectrum of the gun cavity operated at 9 MV/m (see Fig. 8). Accordingly, the largest disturbances occur at 10.3 Hz, 20.6 Hz, 24.6 Hz, 80 Hz and a little less between 130 and 315 Hz. The main contribution is made by the frequency at 24.6 Hz, which can be clearly attributed to the membrane pumps of the entire accelerator. The compressors of the helium liquefier presumably generate the disturbances at 24 and 130 Hz, which are transmitted via the helium transfer line and the basement. However, the source of the 10 and 80 Hz resonance is not known, but the waveguide can be identified as the transmission path. Despite all the disturbances, the overall remaining phase noise across all frequencies is σ_φ=0.02° at 1.3 GHz or σ_φ=45 fs respectively and thus fulfils all requirements. However, due to the so called in-loop measurement method used here, this value only represents the additive phase noise of all elements within the control loop but not the RF reference itself.

Table 2: Lorentz Force Coefficient of Gun II and Comparison with Gun I as well as TESLA 9-Cell Cavities, All for Accelerating Gradient and On-Axis Peak Electric Field, Note: $k_0=k_{acc}(E_0/E_{acc})^2$, E_0/E_{acc}=2.56.

	SRF Gun I	**SRF Gun II**	**TESLA Cavity**
k_{acc} [Hz(MV/m)$^{-2}$]	5	9.7	1
k_0 [Hz(MV/m)$^{-2}$]	0.69	1.5	0.25

Another property of interest is Lorentz force detuning that was simply determined by the frequency shift measured as a function of the accelerating gradient squared. As shown in Table 2 the LF-coefficient is a factor of two higher than expected from gun I. This is particularly surprising because the helium pressure sensitivity, having a value of 150 Hz/mbar is almost exactly the same as for gun I. For a better comparability of the Lorentz force, especially with the well-known TESLA 9-cell cavity, the coefficients are also given for the on-axis peak electric field. This shows that SRF gun II responds not only by twice the frequency shift to a change of the gradient compared to its predecessor but even a factor of six compared to TESLA cavities. For a typical gradient of E_{acc} = 8 MV/m (corresponding to E_0 = 20.5 MV/m) this translates into an overall frequency shift of 650 Hz. Due to the relatively small cavity bandwidth of 200 Hz, this makes a continuous tuning while changing the gradient essential. To increase operational safety, this is done automatically by the Supervisory Control and Data Acquisition (SCADA) system.

ISBN: 978-3-95450-233-2 ISSN: 2673-5504 doi:10.18429/JACoW-SRF2021-TUPTEV001

RF SYSTEM

As already indicated, crucial for the stability and quality of the generated electron beam is an amplitude and phase stable RF field for acceleration as well as a low noise / low jitter locking of the photocathode laser to the RF reference of the accelerator (typ. 1.3 GHz). For this purpose, an analog proportional control loop for amplitude and phase is combined into one controller. A simplified block diagram of the technical implementation are shown in Fig. 9.

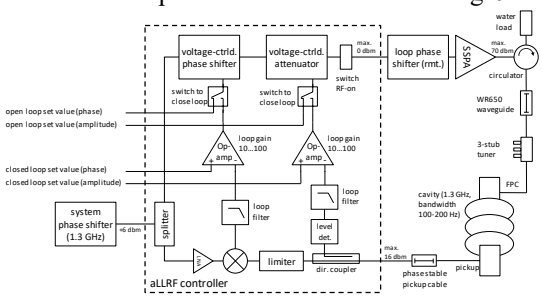

Figure 9: Block diagram of the analog LLRF controller.

According to that, the resonator is driven at 1.3 GHz (generator driven resonator) and both amplitude and phase are continuously adjusted by two actuators (voltage controlled phase shifter and attenuator). The transient signal is taken by a cavity field probe and determined with respect to amplitude (level detector) and phase (mixer). After low-pass filtering both are compared (differential amplifier) with the target value provided by the PLC (Programmable Logic Controller) and SCADA system of the accelerator. The differential voltage determined in this way controls both actuators mentioned before. The stabilized signal is then amplified by a solid state power amplifier (SSPA) and brought to the cavity using a WR650 waveguide. To protect the amplifier, a RF isolator is used to dump the RF power that is reflected by the cavity into a RF load. Additionally, there is also the possibility to adjust the cavity bandwidth by means of a 3-stub waveguide tuner between 50-300 Hz. The overall performance of this 20 years old analog system is still equivalent to that of a modern digital controller and briefly summarized below:

Amplitude Control Loop:
- dynamic range: 40 dB (10000)
- proportional loop gain: 10…100 (typ. set to 100)
- short-term stability: 2×10^{-4} (RMS)

Phase Control Loop:
- dynamic range: ±30°
- proportional loop gain: 10…100 (typ. set to 100)
- short-term stability: 0.01° (RMS, 10 Hz - 10 MHz)

The required RF power is provided by a state-of-the-art SSPA from SigmaPhi Electronics. The amplifier is composed by 10 RF modules that are combined by a WR650 waveguide to reach 15 kW CW RF. The guaranteed minimum small signal gain is 73 dB and the phase drift over an output power range of 2 kW to 15 kW is ≤ 8°. Gain linearity over the same dynamic range is less than ±0.5dB.

The synchronization of the four accelerator cavities, the SRF gun and the photocathode laser with each other is realized using common accelerator references of 13 MHz and 1.3 GHz. These are generated together with other frequencies required for operation by the accelerators master clock called RALAB from LAURIN AG. The time jitter achieved with this setup is summarized in Table 3.

Table 3: RMS Timing Jitter of RF Reference, SRF Gun RF and Laser Oscillator Measured using R&S FSWP Analyzer

	1.3 GHz Reference	SRF Gun RF Field	Laser Oscillator
1 Hz – 10 Hz	75.2 fs	101.3 fs	160.6 fs
10 Hz – 10 MHz	27.3 fs	23.1 fs	85.7 fs
1 Hz – 10 MHz	80.0 fs	103.9 fs	182.1 fs

CONCLUSION

Within the last 6 years, an improved version of the ELBE SRF gun could be commissioned and successfully transferred into user operation. Although the achievable acceleration gradient in daily operation does not reach the design values, it could nevertheless be shown that this novel electron source has made the step from prototype to routine operation in terms of stability, availability and reliability.

ACKNOWLEDGEMENTS

We thank the whole ELBE team for their help with this project. The work was partly supported by the German Federal Ministry of Education and Research (BMBF) Grant No. 05K12CR1 and Deutsche Forschungsgemeinschaft (DFG) project (XI 106/2-1).

REFERENCES

[1] P. Michel, *J. Large-Scale Res. Facil.*, vol. 2, p. A39, 2016.

[2] J. Teichert *et al.*, *Nucl. Instrum. Methods Phys. Res., Sect. A*, vol. 743, p. 114, 2014. doi.org/10.1016/j.nima.2014.01.006

[3] A. Arnold *et al.*, "Fabrication, Tuning, Treatment and Testing of Two 3.5 Cell Photo-Injector Cavities for the ELBE Linac", in *Proc. SRF'11*, Chicago, IL, Jul. 2011, paper TUPO019, pp. 405-407.

[4] A. Arnold *et al.*, *Nucl. Instrum. Methods Phys. Res., Sect. A*, vol. 577, p. 440, 2007. doi.org/10.1016/j.nima.2007.04.171

[5] H. Vennekate *et al.*, *Proc. IPAC'14*, Dresden, Germany, /Jun. 2014, pp. 1582-1584. doi:10.18429/JACoW-IPAC2014-TUPRI015

[6] H. Vennekate *et al.*, *Phys. Rev. Accel. Beams*, vol. 21, p. 093403, 2018. doi.org/10.1103/PhysRevAccelBeams.21.093403

[7] P. Murcek *et al.*, "Modified SRF Photoinjector for the ELBE at HZDR", in *Proc. SRF'11*, Chicago, IL, USA, Jul. 2011, paper MOPO004, pp. 39-42.

[8] A. Arnold *et al.*, "RF Performance Results of the 2nd ELBE SRF Gun", in *Proc. SRF'15*, Whistler, Canada, Sep. 2015, paper THPB055, pp. 1227-1230.

[9] R. Xiang *et al.*, *Phys. Rev. Accel. Beams*, vol. 17, p. 043401, 2014. doi.org/10.1103/PhysRevSTAB.17.043401

[10] A. Arnold *et al.*, "Commissioning Results of the 2nd 3.5 Cell SRF Gun for ELBE", in *Proc. LINAC'14*, Geneva, Switzerland, Aug.-Sep. 2014, paper TUPP066, pp. 578-580.